Czech Technical University in Prague,
Faculty of Nuclear and Physical Engineering

Department of Physics Area: Nuclear Engineering
Focus: Experimental nuclear physics

Spectra in pˇrˇıˇcn´e momentum and correlations from the blast wave model with resonances

Transverse momentum spectra and correlations in the blast wave model with resonances

BACHELOR´S THESIS

Elaborated: V´aclav Koˇsaˇr
Head of the study: Dr. Boris Tom´aˇsik, Department of Physics
Year: 2010

Before the wedding, instead of this page enter the assignment with the signature of the dean (will be the only two-sided letter in your copy) !!!!

Prohlášení

I declare that I have prepared my bachelor thesis independently and I have used only the materials (literature, projects, software, etc.) listed in the attached list.

I have no obvious reason against the use of this complete work within the meaning of Act No121/2000 Coll., on Copyright, on Rights Related to the Copyright Law and on Amendments to Certain Acts (the Copyright Act).

In Prague on ....

....

Václav Košař

Subsection

I would like to thank Dr. Boris Tomášik for his excellent guidance of my Bachelor's thesis, for his patience and for all the time spent explaining the issues, evaluating our work and uppoint out the mistakes and errors I have made.

Václav Košař

The name of the work:

Spectra in pˇrˇıˇcn´e momentum and correlations from the blast wave model with resonances

Author: V´aclav Koˇsaˇr

Branch: Nuclear engineering

Type of action: Bakal´aˇrska pr´ace

Head of the study: Dr. Boris Tomášik, Department of Physics
Department of Physics, Faculty of Nuclear and Physical Engineering, Czech Technical University in Prague

Consultant: -

Abstract: Pr´ace is a re´ser´e of the theory concerning the behaviour of states of matter with high energy density, which is produced by the collision of three low ions at energies higher than GeV per nucleon. The book contains basic information on the extreme state of matter called the quark-gluon plasma, an introduction to quantum statistical mechanics and an introduction to the theory of the boost-invariant expanding fireball of hadronic matter.

The particular object of interest is the Blastwave model with included resonances, whose basic assumptions are the underlying boost-invariant expansion, the over-expansion and the existence of a specific superplane in spacetime, on which the hadronic matter is released from the fireball in a jump.

In the last part of the paper the author fits the two most important parameters of the model

Blastwave by by edited by program DRAGON [B. Tomasik, Comp.Phys.Commun. 180 (2009) 1642-1653] on the spectra in the forward momentum obtained from the STAR experiment.

Kl´ıc´s words: ultrarelativistic cores, sub-black boost-invariant expanding fi- reball, Blastwave model, spectra in the forward momentum, DRAGON

Title:
Transverse momentum spectra and correlations in the blast wave model with resonances
Author: V´aclav K o ˇ s a ˇ r

Abstract: This thesis provides a review about the basics of theories of properties of matter with high energy density, which originates in heavy ion high energy collisions (GeV/nucleus). Basic information about the extreme state of matter called quark- gluon plasma, introduction to quantum statistical mechanics and introduction to theory of longitudinally boost-invariantly expanding fireball of hot matter are men- tioned.
Particular intention is given to the blast-wave model with resonances, whose basic assumptions are longitudinally boost-invariant expansion, transverse expansion, and the existence of a particular hypersurface in space-time, on which hadronic matter abruptly decouples from fireball.
In the final part two most important parameters of the blast-wave model are extracted from fits to the transverse momentum spectra obtained from STAR experiment, using a modification of the program DRAGON [B. Tomasik, Comp.Phys.Commun. 180 (2009) 1642-1653].

Key words: ultrarelativistic nuclear collisions, logitudinally boost-invariant expanding fireball, Blastwave model, transverse momentum spectra, DRAGON

Table of Contents

Introduction

The nucleus of the third ion behaves roughly like a drop of liquid with pˇribliˇznˇe homogeneous goose- total, in the rest frame pˇribliˇznˇe spherically symmetrically distributed around the body. When we observe high-energy collisions (from 1GeV per nucleon) of two three ions, even at the more central entrance of the collision, there is a lower expansion due to the quan-
these phenomena - the nuclei are more and more the "sight". In the area of the pathway in the case of the „heart
the nuclear liquid is strongly undergrown due to the interaction of extreme conditions - the nuclear liquid is strongly undergrown
pic. If the energy density reaches the necessary values, the formation of a hypo- tetic quark-gluon plasma can occur. The quark phenomena cause the transfer of part of the energy of this very dense drop of nuclear matter to the formation of a particle-antiparticle pair, and the considerable pressure causes their overexpansion.

Thus, a fireball of many ˇc´asticˇc´asteˇs is created, expanding more and more substantially into space. As the fireball expands, its energy density decreases, and this causes two significant reverse transitions. First, from a quark-gluon plasma to a hadronic
Gas. This transition is called hadronization. Hadron gas is still sufficiently dense, strongly interacting, so that it can be considered as approximately thermalized.

Next, there is a transition from dense hadronic gas to free hadrons. This transition is called freezing. As the fireball continues to expand, the energy density continues to decrease and the unstable particles decay. We then detect only the more stable particles and try to reconstruct from them the physics of the original nuclear core - the equations of state for the critical states of matter (i.e. The nature of the collective behaviour of dense nuclear matter), the laws of elementary interactions at high energies, the behaviour of a highly excited vacuum.

The question is how to choose a model to describe the high-energy interaction of two three ions and how to choose its parameters. One of the many models is the Blastwave model, whose basic assumptions are the presence of a boost-invariant expansion, an overexpansion and the existence of a specific superplane in spacetime at which the hadronic matter is released in a jump from the fireball. The author of this paper attempts to find the best choice of the two main parameters of this model by means of the DRAGON program [9], which includes the effect of resonances, by fitting the spectra in the forward momentum.

Chapter 1

Contemporary´ view of the structure masses

1.1 Element´arn´ı ˇc´astice

The elementary unit of matter is the elementary particle, which is an indivisible object with certain physical properties. Under certain circumstances, stable structures are formed over a period of time, which can be divided according to the degree of elementarity into: cell, molecule, atom, shell and nucleus.

An atom is made up of a shell and a nucleus. The shell of the atom consists of electrons in an arrangement determined by electromagnetic interaction with an oppositely charged nucleus. The nucleus is composed of nucleons - protons and neutrons, whose constituents are a triplet of quarks.

In the last century it has become apparent that nature is not limited to protons, neutrons and electrons, but is made up of a much larger group of particles, which are in turn made up of a relatively small group of quarks and leptons. This idea is called the standard model, which, together with quantum chromodynamics, quantum electrodynamics, where interactions are mediated by a powerful intermediate particle, constitutes the basis of modern particle physics.

1.2 Standard model

We divide the elementary particles of the standard model into three groups - quarks, gluons and intermediate bosons. For each particle there is also a antiparticle, pˇriˇcemˇz in some cases the particle and the antiˇc particle are indistinguishable. We divide quarks and leptons into three generations, the first one being stable and the other two being unstable excitations decaying with weak interaction on the first generation elementary particle.

Quarks are carriers of the colour charge of the strong interaction. There are stars in the bound state to other quarks, so that „the "set" of colours was **neutral**. Therefore, quarks form stars hadron: either a baryon, in which all three quarks have a different colour, or a meson, in which which is a quark and an antiquark, i.e. a colour and its anti-colour. Theoretically, the following have been determined and more complex structures such as the pentaquark, which is composed of four quarks and one antiquark.

Quarks never occur individually but are embedded in the hadron together with other quarks. If we tried to pull two quarks apart, their potential energy would grow linearly with their distance. The properties of the gluon, the boson that mediates the strong interaction, play a very important role here. The gluon is immaterial and has a strong interaction charge, which makes it easy to form and interact with other gluons. Eventually, as the quark is pulled away, the binding energy increases sufficiently to give rise to a quark-antiquark pair. This recombines with the original quarks that were pulled away and we have both quarks back in the bound state.

The interaction between the particles is mediated by intermediate bosons. This means that the energy and momentum are transferred in quanta by intermediate bosons, which exist often very shortly, and so due to the uncertainty principle their mass has a certain uncertainty.

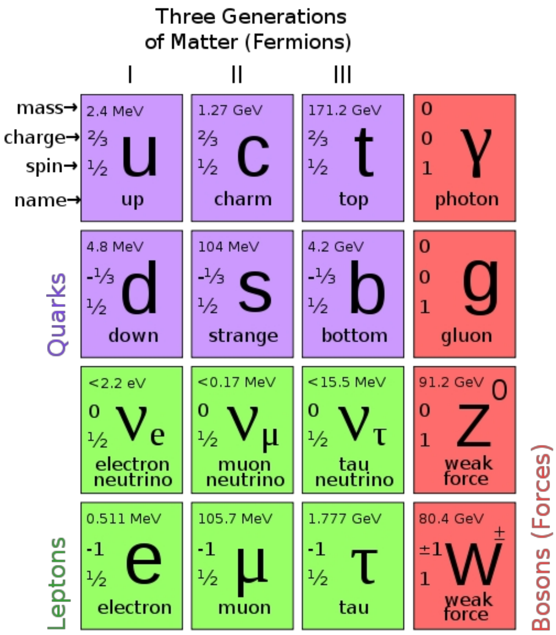

Figure 1.1: Elementary part of the Standard Model. [11]

1.3 Quark-gluon plasma

The quark-gluon plasma, abbreviated QGP, is a state of matter governed by the theory of quantum chromodynamics (QCD). The original proposition concerning the quark-gluon plasma is
[14]. If the matter - hadronic gas is condensed into a volume of sufficient energy density
gies [1GeVfm^{-3}], the quarks of different hadrons find themselves close enough to each other, they are destined to be exclusively bound to their hadronic triple or pair and can
to move freely. Thus, if we can say that „shared" with each other

to individual hardons becomes meaningless, then we call this state quark-gluon with plasma.

However, no theory can do without experimental facts and therefore we need a device for QGP production. We expect that if we have a sufficient energy ratio of two ions tˇeˇzk of an element, we will achieve the necessary energy density for the existence of a QGP phase for a period of about 10^{-23} s. We call such a collision the *Little Slice*. By the nature of the QGP, it is impossible to investigate it directly, but by observing the emergence of more hadrons we could learn a lot about this state. For this purpose, accelerators and particle detectors are able to measure the edge energy needed for QGP formation and can efficiently observe the produced particles

1.4 QGP and Velky´ tˇresk

In the large volume theory we consider the dissolution of a large amount of matter from a state of high density. If the theory is consistent with reality, the matter must have passed through the QGP state within $10\mu s$ after the onset of the Big Bang If we can investigate this state of matter sufficiently, we will gain further insights into the origin of the universe. The problem lies in some of the differences between the *Big Bang*, from which the universe originated, and the *Little Bang*, which we can create at the accelerator

1. *Much faster hadronization of the fireball of Mal´e tesko*

   While for the Big Bang we assume that the expansion of the QGP fireball is slowed down by the gravitational acceleration of a huge amount of accumulated matter, for the Little Bang we consider the expansion into the vacuum. We can derive the characteristic hadronization times of the QGP of the Large Mass Spectrum at $\tau_{bb} = 10$ µs and of the Small Mass Spectrum at $\tau_{mb} = 10^{-17}\ \mu s$.

2. *Nonzero baryon force in the fireball of Mal´e tesko*

   In the post-atomic universe, the baryon force was practically zero, unlike in the ex-perimeter. The asymmetry between matter and antimatter at the acceleration
   is described by the ˇtight baryon equation $B = N_B - N_{B^-}$. Ideally
   $B = 0$. In the case of a collision, we produce antiparticle-antiparticle pairs, and thus the number of detected particles N grows while B is maintained, or at least B/N 0. The problem of asymmetry can theoretically be overcome by extrapolation of the baryon chemical potential In addition, by increasing the energy of the interface we increase the number of pairs formed.

3. *Much higher energy density.*

   According to the Big Bang theory, the universe evolves from a continuous singularity characterized by, among other things, infinite density and temperature. By studying the accelerator we can only reach finite values.

Chapter 2

Quantum statistical mechanics

2.1 Quantum statistical mechanics

We define the *density matrix* as a self-consistent, positive operator with unit hundred.

$$\hat{\rho}^* = \hat{\rho} \qquad \forall |\psi> \in \mathrm{H} <\psi|\hat{\rho}\psi> \geq 0 \qquad \mathrm{Tr}\,\hat{\rho} = 1$$

The density matrix can be defined using the positive terms w_j and the vector $\psi_j \in \mathrm{H}$ next

$$\hat{W} = \sum_j w_j \frac{|\psi_j><\psi_j|}{<\psi_j|\psi_j>} \qquad \hat{\rho} = \frac{\hat{W}}{\mathrm{Tr}\,\hat{W}}. \tag{2.1}$$

Therefore, using the density matrix we can also calculate the *mean value of the observable* $\hat{O} = \hat{O}^*$:

$$\bar{O} = \sum_j w_j \frac{<\psi_j|\hat{O}\psi_j>}{<\psi_j|\psi_j>} = \mathrm{Tr}[\hat{\rho}\hat{O}].$$

In this example we will use the natural units $k = c = k_B = 1$.

2.2 The truest difference between the Grandkano-nicky´ file

Let us have a quantum system described by two commuting operators $\hat{H}$, $\hat{B}$, i.e. hamiltonian and baryon čísle. Since we will be working with general states and not just the eigenstates of the baryon force operator, we will actually be building a grand canonical statistical ensemble where the baryon force is not fixed

Let the Hamiltonian have a discrete spectrum $\hat{H}\hat{P}_j = E_j \hat{P}_j$, where $\hat{P}_j$ is an orthogonal projector onto the proper subspace. Let us define the common set of orthogonal projectors on their own subspaces $\{\hat{P}_l \mid \hat{H}\hat{P}_l = E_l \hat{P}_l \wedge \hat{B}\hat{P}_l = b_l \hat{P}_l\}$.

Let us now consider a statistical ensemble of states with different values of the baryon pressure and energy, which we describe by means of the density matrix:

$$\hat{\rho} = \sum_l w_l \frac{\hat{P}_l}{\mathrm{Tr}\,\hat{P}_l},$$

where p´ad´ad´ame assumes that $\dim \hat{P}_l = \mathrm{Tr}\,\hat{P}_l < +\infty$.

We know the mean values of the energy $\bar{E}$ and the baryon $\bar{b}$:

$$\bar{E} = \mathrm{Tr}[\hat{\rho}\hat{H}] = \sum_l w_l E_l \qquad \wedge \quad \bar{b} = \mathrm{Tr}[\hat{\rho}\hat{B}] = \sum_l w_l b_l.$$

Let us now ask what is the nejpravd˘epodobn˘ej˘s density matrix, or equivalently what is the nejpravd˘epodobn˘ej˘s difference between finding different values of the energy and the baryo-new force. Introduce entropy:

$$S = -\,\mathrm{Tr}[\hat{\rho}\ln\hat{\rho}] = -\sum_l w_l \ln w_l$$

and we will maximize it for the given conditions, for $\bar{E}$, $\bar{b}$.

$$\Lambda(w_1, w_2, \ldots) = -\sum_l w_l \ln(w_l) + \alpha \sum_l w_l - \beta \sum_l w_l E_l + \ln\lambda \sum_l w_l b_l, \tag{2.2}$$

where β, $\ln\lambda$ are Lagranger multipliers. Sometimes we denote $e^{\beta\mu} = \lambda$ as fugacity, where μ is the baryon chemical potential.

Let us look for an option w_j so that the function $\Lambda(w_1, w_2, \ldots)$ has a maximum in it. Because

$$\partial^2 \Lambda(w_1, w_2, \ldots) = -\sum_l \frac{1}{w_l} < 0 \text{ on } w_l \in (0, 1)$$

lies the maximum at the stationary point of the function - i.e. at the point where w_l is satisfied

$$\forall l \quad \partial_{w_l} \Lambda = 0.$$

We're getting a lot out of it:

$$w_l = Z_G^{-1} e^{-\beta(E_l - \mu b_l)} = \langle l | Z_G^{-1} e^{-\beta(\hat{E} - \mu\hat{B})} | l \rangle,$$

where $Z_G = e^{\alpha - 1} = \sum_l e^{-\beta(E_l - \mu b_l)}$ is called the partition function.

And so we have enough:

$$\bar{E} = -\partial_\beta \ln Z_G \qquad \bar{B} = -\frac{1}{\beta}\partial_\mu \ln Z_G. \tag{2.3}$$

For the density matrix in this state we have

$$\hat{\rho} = \frac{e^{-\beta(\hat{H}-\mu\hat{B})}}{\mathrm{Tr}\, e^{-\beta(\hat{H}-\mu\hat{B})}}.$$

For the partition function we have

$$Z_G = \mathrm{Tr}\, e^{-\beta(\hat{H}-\mu\hat{B})} = \sum_n <n|\, e^{-\beta(\hat{H}-\mu\hat{B})}\, |n>. \tag{2.4}$$

Since Tr is representationally invariant, we can use any ortho-normal basis. This allows us to learn a basis of occupation rules for non-interacting particles. Interaction is then sometimes introduced by means of fault development.

2.2.1 Bosons and fermions

Consider a system of indistinguishable and non-interacting particles described by two commuting operators, the Hamiltonian $\hat{H}$ and the baryon operator $\hat{B}$. Let the single-valued hamiltonian $\hat{H}_{(1)}$ take only discrete values $\hat{H}_{(1)}\, j >= \epsilon_j\, j >$, where $j >$ is an eigenvector. On the Fock space we introduce a symmetrized or antisymmetrized basis of the containment elements

$$\{|(S/A), n_1^{(b)_1}, n_2^{(b)_2}, n_3^{(b)_3} \ldots >,$$

where $n_i^{(b^{i})}$ are the occupation numbers of the single-variable states $|i>$, for which $\hat{H}_{(1)}\, |\, i >= \epsilon_j\, |i> \wedge \hat{B}\, |\, i >= b_i\, |i>\}$.

For the total Hamiltonian (Fock space) and baryon space we get

$$\hat{H}|(S/A), n_1^{(b^1)}, n_2^{(b^2)}, n_3^{(b^3)} \ldots >= \sum_i n_i^{(b^i)} \epsilon_i\, |(S/A), n_1^{(b^1)}, n_2^{(b^2)}, n_3^{(b^3)} \ldots >,$$

$$\hat{B}|(S/A), n_1^{(b^1)}, n_2^{(b^2)}, n_3^{(b^3)} \ldots >= \sum_i n_i^{(b^i)} b_i\, |(S/A), n_1^{(b^1)}, n_2^{(b^2)}, n_3^{(b^3)} \ldots > .$$

For the construction of the grand canonical set we use formula (2.4), which has the form in our chosen base:

$$Z_G = \sum_n e^{-\sum_{i=1}^{\infty} n_i \beta(\epsilon_i - \mu b_i)} = \sum_n \prod_i e^{-n_i \beta(\epsilon_i - \mu b_i)}.$$

Because all combinations of the occupation clauses remain (if finally contained, we can change the order of the sum and product. We draw all states with free N total number of particles

$$Z_t = \begin{cases} \prod_i \sum_{n=0}^{\infty} e^{-n_i\beta(\epsilon_i-\mu b_i)} & \text{for bosons.} \\ \prod_i \sum_{n_i=0}^{1} e^{-n_i\beta(\epsilon_i-\mu b_i)} & \text{for fermions.} \end{cases}$$

We add sums (for bosons under the condition that $e^{-n_i\beta(\epsilon_i-\mu b_i)} < 1$)

$$\ln Z^{(t)}_{F+,B-} = \pm \sum_i \ln(1 \pm e^{-\beta(\epsilon_i-\mu b_i)}), \tag{2.5}$$

where the sum is the sum of all single-particle states, the upper sign is valid for fermions and the lower for bosons.

For the mean value of the baryon pressure from (2.3) we have

$$\bar{B} = -\frac{1}{\beta}\partial_\mu \ln Z^{(t)}_{F+,B-} = \sum_i \frac{\text{Would}}{1 \mp e^{\beta(\epsilon_i-\mu b_i)}} \tag{2.6}$$

Hence the Bose-Eistain and Fermi-Dirac divide $\dfrac{1}{e^{\beta(\epsilon_i-\mu b_i)} \mp 1}$ ...the difference between-

If we sum in (2.5) over states with $b_i > 0$ (cs) and states with $b_i < 0$ (antics) and assume that the possible states for ˇc´astics and antiˇc´astics are the same, we get

$$\ln Z^{(t)}_{F+,B-} = \pm \sum_i \ln(1 \pm e^{-\beta(\epsilon_i-\mu b_i)}) + \ln(1 \pm e^{-\beta(\epsilon_i+\mu b_i)}), \tag{2.7}$$

where the sum of $\sum_i$ will now denote the sum of all states with $b_i > 0$. Using $\lambda^{b_i} = e^{\beta\mu b_i} = e^{\frac{\mu}{T}}$ we could modify the previous relation to:

$$\ln Z^{(t)}_{F+,B-} = \pm \sum_i \ln(1 \pm \lambda^{b_i} e^{-\beta\epsilon_i}) + \ln(1 \pm \lambda^{-b_i} e^{-\beta\epsilon_i}). \tag{2.8}$$

By replacing the baryon equation by a lepton equation, we could use the same procedure to derive the equations for leptons. By allowing only the state $b_i = 1$ we obtain a system of ˇc´astics and antiˇc´astics of the same type.

2.2.2 Density of states

We consider a quantum mechanical problem with an ˇc´asticity in an infinitely deep potential well - a box $<0, L> \times <0, L> \times <0, L>$. We introduce periodic boundary conditions (particles on the circle), which allow for transparent boundary conditions and in the later limit $V \to \infty$ the particular boundary conditions will not be essential.

$$\psi(x_i = 0) = \psi(x_i = L)$$

We obtain a periodic wave of similar shape to the de Broglie wave, but the momentum we now have quantum annihilation: The "fineness" of the quantum channel is determined primarily by the size of the box. We have

$$\psi(x) = e^{i\vec{p}\cdot\vec{x}}$$

$$\vec{p} = \frac{2\pi}{L}(k_1, k_2, k_3) \text{ where } k_i \in \mathbb{Z}.$$

Let f be a real function of a real variable, ϵ_n are real numbers. Let's take the sum of

$$\sum_{n=0}^{\infty} f(\epsilon_n) = \int_0^{\infty} d\mu_D(\epsilon) f(\epsilon),$$

where in the integral we generate the measure next

$$d\mu_D(\epsilon) = d \sum_{n=0}^{\infty} \vartheta(\epsilon - \epsilon_n).$$

The measure therefore determines how many "riba" cells there are at a given point ϵ. If there is a function g simply with a continuous non-zero first derivative g' on $< 0, +\infty >$ such that it appropriately approximates trend ϵ_n. So, for example:

$$\forall n \in \mathbb{N}_0 \quad |g(n) - \epsilon_n| < \delta_1 \quad \wedge \quad \forall x \in < n-1, n >: |g'(x) - (g(n) - g(n-1))| < \delta_2,$$

where $\delta_{1,2} > 0$ are sufficiently small. The function can be set to $< 0, +\infty >$ invert and approximate the measure in the previous integral:

$$d\mu_D(\epsilon) \approx d(g^{-1}(\epsilon))$$

$$\sum_{n=0}^{\infty} f(\epsilon_n) \approx \int_0^{\infty} d(g^{-1}(\epsilon)) f(\epsilon) = \int_0^{\infty} d\epsilon \frac{dg^{-1}(\epsilon)}{d\epsilon} f(\epsilon).$$

The preceding procedure can be easily generalized to the following higher-dimensional variant:

$$\sum_{k_1, k_2, k_3 = -\infty}^{+\infty} f(\epsilon(\vec{p}(k_1, k_2, k_3))) \approx \int_{R3} dk_1 dk_2 dk_3 f(\epsilon(\vec{p}(k_1, k_2, k_3))) = \int_{R3} d^3\vec{p} \, J f((\epsilon(\vec{p})),$$

where J is a suitable Jacobian. In the case of a boxed crystal $J = V/(2\pi)^3$. To simplify the procedure, we work with the integral instead of the sum, which is motivated by the fact that in the limit $L \to \infty$ the spectrum of the impulse operator is continuous. We replace the sum of the above procedure by the integral of the following

$$\sum_i [\ldots] = g \int \frac{V d p^3}{(2\pi)^3} [\ldots], \tag{2.9}$$

where, in addition, we generally use the degeneracy factor g, which denotes further degrees of freedom to expand the phase space into further dimensions. We have derived this for periodic boundary conditions or arbitrarily large volumes.

2.2.3 Fermi and Bose ˇc´astic and antiˇc´astic gases of one type

By allowing the state with baryon ˇc´ıc´ıs only $b_i = \pm 1$ in (2.8), we derive the relation for
$\ln Z^{(t)}_{F^+,B-}$ for ˇc´astic and antiˇc´astic gas of one type. If we continue with (2.9), we get mute:

$$\ln Z_{F/B}(V, \beta, \lambda) = \pm gV \int \frac{dp^3}{(2\pi)^3} \ln(1 \pm \lambda e^{-\beta\sqrt{p^2+m^2}}) + \ln(1 \pm \lambda^{-1} e^{-\beta\sqrt{p^2+m^2}}), \quad (2.10)$$

where the upper sign is valid for fermions, the lower for bosons and the ˇc ́ast at λ^{-1} corresponds to antiparticles.

Using the relation for the grand canonical potential

$$\Omega(T, V, \mu) = -PV = -\beta^{-1} \ln Z_t,$$

where P is the pressure, we get

$$P(\beta, \lambda) = \mp g \int \frac{dp^3}{(2\pi)^3} [\ln(1 \pm \lambda e^{-\beta\sqrt{p^2+m^2}}) + \ln(1 \pm \lambda^{-1} e^{-\beta\sqrt{p^2+m^2}})], \quad (2.11)$$

where g is the degeneracy factor, see the conclusion of subsection 2.9, and where the upper sign is valid for fermions, the lower for bosons, and the value at λ^{-1} corresponds to antiparticles.

2.2.4 Photon gas

For the photon gas, we can derive a simple equation of state from (2.11), which corresponds to the theory of blackbody radiation. For the photon gas: $m = 0$, $\epsilon_i = p$, in the integral we omit the antiparticle multiplied by λ^{-1} and set $\lambda^b{}_i = 1$. The last two assumptions are justified by the fact that the photon and the antiphoton are indistinguishable particles. Therefore, the addition of a photon can be interpreted as the addition of an antiphoton, and the chemical potential can be considered to be zero. The feeling for the antiparticle states disappears also due to the indistinguishability. Therefore, by substituting the above assumptions into (2.11), switching to spherical coordinates, and introducing the substitution $x = p/T$, we obtain the equation of state of the photon gas:

$$P = -\frac{4\pi g T^4}{(2\pi)^3} \int_0^\infty dx x^2 \ln(1 - e^{-x}).$$

Because the integral is equal to $-\pi^4/45$ we get

$$P = g\frac{\pi^2}{90}T^4, \quad (2.12)$$

where for photons $g = 2$ (polarization). D ́ıky of the relation resulting from the definitions:

$$\bar{E}(T) = -\partial_\beta \ln Z_t = -\partial_\beta - \beta PV = 3PV$$

Thus, we obtain a relation for the pressure of the radiation (the ultrarelativistic limit for the limbic frequency, i.e. for $p >> m$):

$$P = \epsilon(T)/3,$$

where $\epsilon(T)$ is the energy density of the electromagnetic field. From here we can easily determine the well-known Stefan-Boltzmann constant.

2.2.5 Bag model

The original contribution to this model is [12]. The bag model is a primitive model of the QGP hadronization process. Since we are working with high energies, we can to neglect the masses of all QGP and HG (Hadron Gas) particles due to their Momentum. However, the degeneracy factor is a higher value, which multiplies the dimension of the phase space. We take into account that the phase space of fermions is somewhat smaller than that of bosons due to the Pauli exclusion principle. More precisely, 7/8 times smaller. This is shown in [5] where this example is taken from.

$$g_{QtP} = g_t + \frac{7}{8} \times 2(\text{antiparticle}) \times g_q + g_{EW} \approx 56.5\,,$$

where for the gluons, the quarks:

$$g_t = 2(\text{spin}) \times (N_c^2 - 1)(\text{color}) = 16\,,$$

$$g_q = 2(\text{spin}) \times N_c\,(\text{color}) \times n_f \approx 15$$

,

$$g_{EW} = 2(\gamma) + \frac{7}{8} \times 2(\text{antiparticle}) \times (2(\text{spin}) \times 2(e + \mu) + 3(\nu_e L \nu_\mu L \nu_\tau L)) = 14.25.$$

We're replanting: $N_c = 3$(number of colors), $n_f \approx 2.5$ (effective number of waves). For ν we only consider left-handed neutrinos and right-handed antineutrinos and do not assume tau production.

We estimate the hadronic gas in the zero point by the pion gas and add the electroweak particles

$$g_{Ht} = 3(\pi^+ \pi^- \pi^0) + g_{EW} \approx 17.25.$$

During hadronization, both HG and QGP pressures are equal, therefore:

$$P_H = g_{QtP} \frac{\pi^2}{90} T_H^4 - B = g_{Ht} \frac{\pi^2}{90} T_H^4. \qquad (2.13)$$

From the pressure for the photon gas modelling the QGP we subtract the so-called bag constant

$B^{\frac{1}{4}} \approx 190$MeV obtained by fitting the experimental data, this constant is re-presents the latent heat QGP. If we did not introduce this constant, then $P_{QtP} > P_{Ht}$ would always be valid and matter would be constantly in a quark-gluon plasma state. We can also think of the constant B as the pressure that pushes the

physical vacuum to
proton hold it together." We thus estimate the temperature of
and hadronization:"

$$T_H = B^{\frac{1}{4}} \left(\frac{90}{\pi 2 \Delta g} \right)^{\frac{1}{4}} \approx 130\text{MeV}.$$

Another possibility to determine T_H is to use the formula for the radiation pressure (ultra-relativistic limit) and the energy density:

$$P = \frac{\epsilon}{3}.$$

Since the proton is the most abundant quark system, we can estimate the energy density at hadro-nization as:

$$\epsilon_H = \frac{m_p}{(1\mathrm{fm})^3} = 1\mathrm{GeVfm}^{-3}.$$

Then, by substituting the energy density into the Boltzmann relation, we obtain the pressure with which we can estimate the hadronization temperature:

$$T_H = 160\mathrm{MeV}.$$

Chapter 3

Sub-black boost-invariant expanding fireball

3.1 Notes

1. I use formulas in the text:

   $$\delta(f(x)) = \sum_i \frac{\delta(x - x_i)}{|f^r(x_i)|}$$ where the sum of bˇeˇz′ı pˇres points where f (x) is zero (3.1)

   and makings

   $$\delta^+(f(x)) = \vartheta(x)\delta(f(x)) \tag{3.2}$$

2. For the ˇctyˇr vector, we often denote by $a^\mu = a$, without emphasis, that it is a ˇctyˇr vector. However, I use the symbols a and $_\mu^\mu = a^2$. I denote the three-dimensional vectors by $\vec{a}$.

3. A frequently used formula for the fourth-order stability of the crystal is:

   $$p^2 = E^2 - \vec{p}^{\,2} = m^2 \tag{3.3}$$

   therefore for the following defined Dp

   $$Dp = 2\delta^+(p_\mu p^\mu - m^2)d^4p = \frac{dp^3}{E} \tag{3.4}$$

3.2 Coordinates

3.2.1 Spatiotemporal coordinates

The following coordinates are suitable to describe the sub-black boost invariant expansion:

Let us define the super-surface on which we define the frost. We leave it as a general superplane in the fourth space. In the Blastwave model we then introduce a more specific definition.

Above the surface of the frost:

$$\sigma = \{x^\mu \mid \text{superplane in 4-dimensional space}\} \quad (3.5)$$

But we will introduce quantities that we will use to describe the individual frequencies of the expanding fireball in the laboratory system.

Spatial vector of the fourth part of the fireball in the laboratory system

$$x^\mu = (t, x, y, z) = (t, \vec{x}) \quad (3.6)$$

Cˇtyˇthvelocity of the expelling fireball with positional x^μ :

$$U^\mu = \frac{dx^\mu}{d\tau} = \frac{(V_0, \vec{V})}{\sqrt{1 - V_0^2 - \vec{V}^2}}. \quad (3.7)$$

3.2.2 Co-ordinates of the ˇc´astice

For the description of a particle in a laboratory system we define the following values

Cˇtyˇtyˇc´asticity:

$$p^\mu = (p^0, \vec{p}) \quad (3.8)$$

The speed of the acceleration is inferior:

$$y = \frac{1}{2} \ln \frac{p^0 + p_z}{p^0 - p_z} \quad (3.9)$$

The velocity of the particle in the laboratory system

$$\vec{v} = \frac{\vec{p}}{p^0} \quad (3.10)$$

Vector of the pˇr´ı´ıc´ıc´ıc´ı momentum of the axis:

$$\vec{p}_t = (p_x, p_y) = p_t (\cos \varphi, \sin \varphi) \quad (3.11)$$

Pˇr´ıˇc´ıc´ıc´ı mass of the asterisk:

$$m_t = \sqrt{m^2 + p_t^2} \quad (3.12)$$

Energy of the particle in the laboratory system:

$$E = p^0 = \sqrt{m_t^2 + p_z^2} = \sqrt{m^2 + p_t^2 + p_z^2} \quad (3.13)$$

Energy of a particle in the local system x^μ :

$$E^* = \frac{1}{\sqrt{1 - V^2}} (p^0 - \vec{V}\vec{p}) \quad (3.14)$$

We can easily see that it pays:

$$p^\mu = (m_t \cosh y, p_t \cos \varphi, p_t \sin \varphi, m_t \sinh y), \quad (3.15)$$

$$E^* = p\, u_\mu{}^\mu\,. \tag{3.16}$$

3.3 Hydrodynamic description of the relativistic relation

In the hydrodynamic description of the relativistic relation, we introduce the following signs

Density of the number of ˇc´astic:

$$n(\vec{x}, t)d^3x = n(x^\mu)d^3x = \text{poˇcet ˇc´astic v volume } d^3x \text{ v ˇcase t.} \tag{3.17}$$

Total number of ˇc´astic in ˇcase t:

$$N^{(t=kost)} = \int d^3x\, n(x)^\mu \tag{3.18}$$

In general, we do not have to restrict ourselves to a superplane in spacetime defined by some value of time, but we can determine the number of worlds passing through a general superplane in spacetime. The calculation must be carried out in a more complex way. This is usually done in some models of relativistic relations, where we define a freezing superplane, which we then integrate over. On this topic, see also Subsection 3.5.

Current ˇc´astic:

$$\vec{j}(\vec{x}, t) = \vec{j}(x)^\mu \tag{3.19}$$

is a vector such that for any infinitesimal element of the surface $d\vec{S}$ at the point $\vec{x}$ it gives the scalar product $d\vec{x}\,\vec{j}(\vec{x}, t)$ of the number of particles passing through the given element in time dt.

Cˇthˇrstream:

$$j^\mu = (n(\vec{x}, t), \vec{j}(\vec{x}, t)) \tag{3.20}$$

Cˇaspatial distribution of ˇc´astic:

$f(x^\mu, p^\mu)d^3x d^3p$ = the number of particles in the phase volume $d^3x d^3p$ at the point (x^μ, p^μ) (3.21) follows from here:

$$n(x^\mu) = \int d^3p\, f(x^\mu, p^\mu), \tag{3.22}$$

$$\vec{j}(x^\mu) = \int d^3p\, \vec{v} f(x^\mu, p^\mu). \tag{3.23}$$

Because the particles are located on the mass shell - i.e. $p^0(\vec{p}) = \sqrt{p^2 + m^2} = E$, it follows from here by the formula (3.4):

$$j^\nu(x^\mu) = \int_{p^0=E} d^3p \frac{p^\nu}{p^0} f(x^\mu, p^\mu) = \int Dp\, p^\nu f(x^\mu, p^\mu). \tag{3.24}$$

Hence the d´ ale for $p^0 = E$:

$$E\frac{d^3j^\nu}{d^3p}(x^\mu, \vec{p}) = p^\nu f(x^\mu, p^\mu), \tag{3.25}$$

$$E\frac{d^3N^{(t=bone)}}{d^3p}(t, \vec{p}) = \int d^3x\, E f(x^\mu, p^\mu). \tag{3.26}$$

However, the previous formula is valid only for the integration over the spacetime plane from constant time. More generally, the worlds are calculated and the procedure is more complex. See Section 3.5.

3.3.1 Differences in the axis

For the description of the difference of particles in spacetime we use the Lorentzian invariant difference, which is a generalization of the non-relativistic difference, which is invariant under the Galilean transformation. This satisfies the requirement that the higher transformed momentum spectrum corresponds in all systems to a higher invariant representing the frequency of occurrence of the particle energy in a given system, i.e. $\sqrt{p^2 + m^2}$. The invariance is easily obtained by trans-forming the differential equation of the component of the uncertainty p and by applying the modified formula for the energy. The total number of particles on the chosen space-time superplane is N.

Lorentz invariant distribution:

$$E\frac{d^3N}{d^3p} = p^0\frac{d^3N}{d^3p} = \sqrt{p^2+m^2}\frac{d^3N}{d^3p}(p) \tag{3.27}$$

Production function:

$$S(x, p) \quad \text{such that} \quad E\frac{d^3N}{d3p} = \int d^4x\, S(x, p) \tag{3.28}$$

Local Boltzmann difference:

$$f(x^\mu, \vec{p}) = \frac{d3j0}{d3p} \propto n(x^\mu)\exp(-E^*/T), \tag{3.29}$$

where E^* is replaced by (3.14).

3.4 Bjorken's boost invariant expansion

At very high energies, we can use the phenomenological model of the divergent invariant expansion, in which the separation of the produced particles with a given rapidity is approximately uniform in the region between the rapidities of the original particles y_0. [2] i.e:

$$\frac{dN_B}{Always} = \begin{cases} N y^{-1} & \in < -y_0, y_0 > \\ 0 & \text{otherwise.} \end{cases}$$

As a consequence, in the limit of $y_0 \to \infty$ the expansion (even too high) occurs in the same way in each system of the set of systems mutually boosted, i.e. in each such system the difference has the shape given by the above relation. The only problem with which we have to deal with is the finality of y_0. We can assume that for boosts in the region of medium rapidity $y = 0$ we approximately achieve uniformity.

free

3.5 Differences in momentum during

zing

„small

The original work concerning this subsection is [1]. We assume that freezing occurs in every system in the same *sub-black proper case*, i.e. at $\tau = \tau_{fo}$. Thus, we do not consider the contribution to the *eigentime* due to the *boost-invariant* expansion, which is consistent with the *boost-invariant* expansion *of the fireball*.

Intuitively, we would assume that in order to obtain the difference between the particles, it is sufficient to integrate the invariant difference over the *freezing surface* (3.43):

$$E\frac{dN^3}{d3p} = \int_\sigma E^* f(x^\nu, p^\nu) = \int_\sigma at\, p_\mu^\mu f(x^\nu, p^\nu),$$

but this assumption is wrong. Such a definition would violate the law of conservation of energy. This can be proved after the integration of EdN. [1].

Let us define an element of a superplane as a vector which has a norm equal to the surface of the superplane and is a quartic perpendicular to it:

$$d\sigma_\mu = \varepsilon_{\mu\nu\nu_1\nu_2\nu_3} \partial x_\alpha^{\nu_1} \partial x_\beta^{\nu_2} \partial x_\gamma^{\nu_3}\, d\alpha d\beta d\gamma,$$

where α, β, γ are the coordinates used to parameterize the superplane. Consider now the number of worldlines that intersect the hyperplane σ at point x^μ and have momentum close to p^μ :

$$dN(\sigma, x^\mu, p^\mu) = f(x^\mu, p^\mu) d\sigma_\mu(x^\mu) p^\mu Dp = d\sigma_\mu(x^\mu) \frac{d3j\mu}{d3p}(x^\nu, \vec{p}) d^3 p, \qquad (3.30)$$

where Dp comes from (3.4) and the second equality follows from (3.25).
meets the requirements of the theorem, let us discuss two choices of hyperplane:

$$d\sigma_\mu^{(z=kost)} = (0, 0, -dxdydt), \qquad d\sigma_\mu^{(t=kost)} = (dxdydz, 0, 0, 0).$$

$$dN = \begin{cases} dxdydz \frac{d^3n}{d3p}(x^\nu, \vec{p}) d^3 p = \text{number of častic in the phase volume } d^3x d^3p \\ dxdydt \frac{d_z}{d3p}(x^\nu, \vec{p}) d^3 p = \text{the number of numbers of particles which flow through the area } dxdy \text{ for čas } dt \text{ and } p^r \in (p \pm dp). \end{cases}$$

From here we can easily go to the general form of the decomposition $d\sigma_\mu = c_\mu^\nu d\sigma_\nu^{(x=konst)}$ where $c c_\nu^\nu = 1$ determines the unit normal to the hyperplane at point $x^{\bar{\mu}}$. Overall, we have

$$d\sigma\, p_\mu^\mu = [c\, p_\mu^\mu] d\sigma = \sum_\nu c^\nu [n_\mu p^{(\nu)\mu}] d\sigma = \sum_\nu c_\nu [d\sigma_\mu^{(x^\nu = kost)} p^\mu],$$

where $n^{(\nu)}$ are unit vectors in the direction of the ν axes. This verifies that (3.30) is the number of worldlines that intersect the hyperplane σ at point x^μ and have momentum close to p^μ.

Let's now modify the formula for dN into the form of an invariant distribution by applying the formula for Dp
(3.4) and for the second equality (3.25) and we get

$$E\frac{d3N^{(\sigma)}}{d3p} = \int_\sigma d\sigma\, p_\mu^\mu f(x^\nu, p^\nu) = \int_\sigma d\sigma_\mu \frac{d3j\mu}{d3p}(x^\nu, \vec{p}). \qquad (3.31)$$

For the production function (3.28) we get

$$S(x, p)d^4 x = d\sigma_\mu (x)p^\mu f(x, p). \tag{3.32}$$

3.6 Symmetrization of the production function, parameterization

We will now review the theory of the effect of symmetrization for indistinguishable bosons on their pro- duction functions, but we will not further investigate the data related to this part.

Due to the properties of indistinguishable particles, the amplitude A_N of the production of particles is symmetric or antisymmetric in the momentum of the produced pairs. Let us consider the amplitude of the production of an N-ˇc´astic system with momenta p_i^μ arising at five points x_i^μ, where $i \in \{1, 2 \ldots N\}$. Then due to symmetry and antisymmetry, respectively, the truth of the formation of a system of particles with momenta p_i^μ in the region G of the following

$$A_N(p_i^\mu, G) = \int_G d^{3N}x \sum_{\pi \in S_n} \operatorname{sgn} \pi \tilde{A}\left((p^\mu_{\pi(1)}, x^\mu_1), (p^\mu_{\pi(2)}, x^\mu_2) \cdots (p^\mu_{\pi(N)}, x^\mu_N)\right),$$

$$P_N(p_i^\mu, G) = |A_N(p_i^\mu, G)|^2,$$

where for bosons we consider sgn $\pi = 1$ and for fermions sgn π is the sign of the permutation.

The effect of symmetrization turns out to be significant for a small region G and it had different momentum in ˇr´ades $\Delta p \Delta x \sim$ k. We can investigate this effect for the two-variable axis variant by introducing a correlation function:

$$c(p_1^\mu, p_2^\mu) = \frac{P_2(p_1^\mu, p_2^\mu)}{P_1(p_1^\mu) P_1(p_2^\mu)} = \frac{E_1 E_2 \frac{d N^6}{d^3p_1 d^3p_2}}{E_1 \frac{d^3N}{d^3p} E_2 \frac{d^3N}{d^3p}}. \tag{3.33}$$

If we solve the single-variable spectrum using the production function (3.32), we can derive [6, 7]

$$c(p_1^\mu, p_2^\mu) = 1 + \frac{\left|\int d^4x\, S(x, K) \exp(iqx)\right|^2}{E_1 \frac{d^3N}{d^3p} E_2 \frac{d^3N}{d^3p}} = 1 + \frac{\left|\int d^4x\, S(x, K) \exp(iqx)\right|^2}{\int d^4x\, S(x, p_1) \int d^4y\, S(y, p_2)}, \tag{3.34}$$

where $q = p_2 - p_1$ and $K = \frac{p_1 + p_2}{2}$. We take the so-called smoothness approximation: $p_1 \approx p_2 \approx K$ and proceed to the new coordinates

$$c(p_1, p_2) - 1 = C(q, K) - 1 \approx \frac{\left|\int d^4x\, S(x, K) \exp(iqx)\right|^2}{\left(\int d^4x\, S(x, K)\right)^2},$$

where $c(p_1, p_2) = C(p_1 - p_2, \frac{p_1 + p_2}{2})$.

3.6.1 N´astin derivation of the symmetrization effect

I was inspired by the work [8]. The derivation of the symmetrization effect can be suggested as follows

The amplitude of the production can be thought of as a simple wave function of the trajectory and the formation of the trajectory as a measurement on this function.

Univariate production function

Let us consider a point source, in which a particle in the eigenstate of the momentum operator with a difference $r(p)$ with a phase $\varphi(x_1)$ at the point x_1 independent of its im- pulse can arise. The position of the phase at a certain point is an essential element of this model, because it provides a kind of minimal localization of the origin of an otherwise delocalized de Broglie wave, which we will see later - when centred, it will have a significant effect. In the x-representation we have:

$$< x | \psi > = \int dp\, r(p)\, e^{ip(x - x_1)}\, e^{i\varphi(x_1)} .$$

This can be interpreted as an approximation of the production of a particle arising at a point x_1 with the state phase $\varphi(x_1)$ in the x-representation. Let us now consider a more general source in the pulse with a slowly varying difference function $S = |a(x, p)|^2$, where $a(x, p)$ is the amplitude:

$$< x | \psi > = \int dp \int dx'\, a(x', p)\, e^{ip(x - x')}\, e^{i\varphi(x')} .$$

We can easily proceed to the p-representation, which is more intuitive from the point of view of the naming-production of a particle with a certain momentum, so we denote by $A(p)$:

$$A(p) = < p | \psi > = \int dx'\, a(x', p)\, e^{-ipx'}\, e^{i\varphi(x')} .$$

The locality of the particle can be satisfied here, for example, by an exponential ball around the distributed momentum and later on we can improve the smoothness of the distribution function and thus obtain the same result.

We have squared absolute values and usually a centred plot of a finite time interval. Since there is no reason to prefer a different phase at any point, we will center this quadrant ještě on all choices of the phase function at all points of production:

$$|A(p)|^2 = \int dx' \int dx''\, a(x', p)\overline{a(x'', p)}\, e^{-ip(x'-x'')}\, e^{i(\varphi(x')-\varphi(x''))} .$$

Let us formally reduce the expression of all functions $\varphi(x) :< -\infty, +\infty > \to < -\pi, +\pi >$ to *the integral of the* previous integral.

$$\int_{\{\varphi(x)\}} d\varphi\; e^{i(\varphi(x')-\varphi(x''))} = \delta(x' - x'').$$

The validity of this relation can be formally verified by discretizing the problem or by stating the similarity with the Feynmann integral for the propagator of the system, whose lagrangian
contains only the function, which is the complete time derivative of the function of time and coordinates.
The result will be the same if we use the Feynmann integral for the propagator
with the same start and end time. For the same starting and ending time

the time evolution operator is converted into an identity and the propagator into a delta function.

After the substitution we obtain the complete truth of the production of one particle with momentum
p we get:

$$P_1(p) = |A(p)|^2 = \int dx\, |a(x,p)|^2 = \int dx\, S(x,p). \qquad (3.35)$$

Two-variable production function

Because we have to symmetrize the wave function, we have enough:

$$A(p_1, p_2) = <p_1| <p_2|\psi_1> |\psi_2> + <p_2| <p_1|\psi_1> |\psi_2> =$$

$$= \int dx_1 dx_2\, a(x_1, p_1) a(x_2, p_2)\, e^{-i(p_1x_1+p_2x_2)} +$$

$$+ a(x_2, p_1) a(x_1, p_2)\, e^{-i(p_1x_2+p_2x_1)}\, e^{i(\varphi(x_1)+\varphi(x_2))} =$$

$$= \int dx_1 dx_2\, e^{i(\varphi(x_1)+\varphi(x_2))}\, e^{-i(p_1x_1+p_2x_2)}$$

$$a(x_1, p_1) a(x_2, p_2) + a(x_2, p_1) a(x_1, p_2)\, e^{i(p_1-p_2)(x_1-x_2)}.$$

Using the smoothness of the function $a(x, p)$ in the momenta for $p_1 \approx p_2 \approx K = \frac{p_1+p_2}{2}$ we have

$$a(x_1, p_1) a(x_2, p_2) \approx a(x_1, \frac{p_1+p_2}{2}) a(x_2, \frac{p_1+p_2}{2}).$$

But let us use $|1 + e^{iy}|^2 = 1 + \cos(y)$ and by averaging over the different phases we get:

$$P_2(p_1, p_2) = |A(p_1, p_2)|^2 \approx$$

$$\approx \int dx_1 dx_2\, |a(x_1, K)|^2 |a(x_2, K)|^2 (1 + \cos[(p_1 - p_2)(x_1 - x_2)]).$$

By introducing $q = p_1 - p_2$, using the possibility of cooling and clocking:

$$\int dx_1 dx_2\, S(x_1, K) S(x_2, K)\, e^{+iq(x_1-x_2)}$$

$$= \int dx_1 dx_2\, S(x_1, K) S(x_2, K)\, e^{-iq(x_1-x_2)}$$

$$= \int dx_1 dx_2\, S(x_1, K) S(x_2, K)\, \frac{e^{iq(x_1-x_2)} + e^{-iq(x_1-x_2)}}{2}$$

$$= \int dx_1 dx_2\, S(x_1, K) S(x_2, K) \cos(q(x_1 - x_2)).$$

So do we

$$P_2(p_1, p_2) = |A(p_1, p_2)|^2 \approx \int dx\, S(x, K)^2$$

$$+ \int dx\, S(x, K)\, e^{iqx} \,.^{2} \qquad (3.36)$$

3.6.2 Parameterization

Let us continue with $c(p_1, p_2)$:

$$c(p_1, p_2) - 1 = C(q, K) - 1 \approx \frac{\left| \int d^4x\, S(x, K) \exp(iqx) \right|^2}{(\int d4x\, S(x, K))^2}$$

It turns out that the right-hand side for a reasonable production function is well described by the following Gaussian:

$$C(q, K) - 1 \approx \exp(-q\, q^{\mu\nu} < \tilde{x}_\mu\ \tilde{x}_\nu >), \tag{3.37}$$

where we introduce the marker

$$\tilde{x}_\mu = x_\mu - < x_\mu >, \quad < f(x) > =_K \frac{\int d^4\, xS(x, K)\, f(x)}{\int d4xS(x, K)}.$$

We can easily check the flatness of the following equations based on the definition and equation (3.3). We then use the second of these to further refine the expression.

$$4K\, K_\mu{}^\mu + q\, q_\nu{}^\nu = 4m\, q\, K^2 \qquad {}^\mu{}_\mu = 0$$

and thus

$$q^0 = \vec{\beta} q - \vec{\beta} \quad \text{Where} \quad \vec{\beta} = \frac{\vec{K}}{K0}$$

and therefore

$$C(q, K) - 1 \approx \exp(-q\, q_{ij} < (\tilde{x}_i - \beta_i\, \tilde{t})(\tilde{x}_j - \beta_j\, \tilde{t}) >).$$

By choosing a suitable system, we can simplify the relationship further. The problem is that the system we choose will vary depending on the momentum of the pair of pairs we use. We choose the so-called out-side-long system:

Longitudinal axis: $\rightarrow l$ in the direction of the bundle,

Outward axis: $\rightarrow o$ in the direction of the upper component of a particular K,

Sideway axis: $\longrightarrow$ perpendicular to the first axis.

By choosing these coordinates, we guarantee that $\vec{\beta}\vec{s} = 0$. Therefore, for the central heart

we have symmetry about the $\rightarrow l$ axis, this is true for all the x-branes that are linear in $\tilde{x}_s$ *ide*,

$< \tilde{x}_i\ ,\ \tilde{x}_j >= 0$. Therefore, we introduce the Bertsch-Pratt parametrization of the correlation function:

$$C(q, K) = \exp(-q^2{}_{out} R^2_{out}(K) - q^2{}_{side} R^2_{side}(K) - q^2{}_{long} R^2_{long}(K) - 2q\, q\, R_{outside}{}^2_{ol}(K)),$$

side

R2

Where

R^2_{out}

R^2

(3.38) $=<(\tilde{x}$ $=<\tilde{y}^2>$, (3.40)

$-\beta_\perp \tilde{t})^2$ $_{long}$ $=<(\tilde{z}-\beta_l \tilde{t})^2>$, (3.41)

$>$ (3.39)

$$R_{ol}^2=<(\tilde{x}-\beta_\perp \tilde{t})(\tilde{z}-\beta_l \tilde{t})>. \quad (3.42)$$

These parameters can be measured and compared with the theoretically derived production function.

3.7 Blastwave model

The original works concerning the Blastwave model are [4, 13]. In the Blastwave model, we assume that the fireball velocity in the z-axis direction does not change, i.e., $V_z = const$. The *subzero eigentime*: $\tau = \sqrt{t^2 - z^2}$

The speed of the pod'eln': $V_z = \frac{z}{t}$,

where t, z are components of (3.6) and V_z is a component of (3.7).

This allows us, among other things, to connect the spatial and spatiotemporal velocity.

The subspace velocity: $\eta_s = \frac{1}{2} \ln \frac{t+z}{t-z} = \frac{1}{2} \ln z \frac{1+V}{1-V_z}$

However, in the Blastwave model we define a three-dimensional superplane in the space on which we define the freezing using the underlying proper time. This can be interpreted as meaning that we neglect the contribution to the proper time from the sub-black expansion and assume that the freezing occurs after a certain pˇresnˇe defined proper time.

Above the surface of the frost:

$$\sigma = \{x^\mu \; / \tau = \sqrt{t^2 - z^2} = \tau_{fo} = \text{const}\} \tag{3.43}$$

To describe the sub-black expansion we define:

Increase the speed of the fireball part: $\vec{V}_t = (V_x, V_y) = V_t (\cos \vartheta, \sin \vartheta)$

Pˇrˇıˇcˇıcˇıcˇıcˇırˇıcˇıcˇıpart of the fireball: $\eta_t = \frac{1}{2} \ln \frac{1 + \sqrt{\frac{V_t}{1-V_z^2}}}{1 - \sqrt{\frac{V_t}{1-V_z^2}}}$

With this quantity it is necessary to pay attention to the fact that it is not a higher speed as it is defined. It only occurs in the region of medium rapidity, i.e. $in_z = 0$.

Radial coordinate of the fireball part: $r = \sqrt{x^2 + y^2}$,

where x, y are the components of (3.6) and $V_{x,y}$ are the components of (3.7).

Using the previous assumptions, we derive the following equations for the four vectors x^μ and u^μ defined in (3.6) and (3.7) describing the parts of the expanding fireball:

$$x^\mu = (\tau \cosh \eta_s, r \cos \vartheta, r \sin \vartheta, \tau \sinh \eta_s), \tag{3.44}$$

$$dx^\mu = \tau r d\vartheta d\eta_s \, d\tau dr, \tag{3.45}$$

$$u^\mu = \frac{1}{\sqrt{1 - (V_t^2 + V_z^2)}} (1, V_t \cos \vartheta, V_t \sin \vartheta, V_z), \tag{3.46}$$

$$u^\mu = (\cosh(\eta_s) \cosh(\eta_t), \cos(\vartheta) \sinh(\eta_t), \sin(\vartheta) \sinh(\eta_t), \sinh(\eta_s) \cosh(\eta_t)), \tag{3.47}$$

$$The_z = \tanh \eta_s . \tag{3.48}$$

$$V_t = \frac{\tanh \eta_t}{\cosh \eta_s} \tag{3.49}$$

We can easily see that it is valid:

$$E^* = p\, u_\mu^{\ \mu} = (m_t \cosh(\eta_s - y) \cosh(\eta_t) - p_t \sinh(\eta_t) \cos(\varphi - \vartheta)). \tag{3.50}$$

Let us use the $d\sigma\, p_\mu^{\ \mu} = \tau\, r m_{fot} \cosh(\eta_s\ y) d\eta_s$ drdφ, which follows from the properties of the above- surface. We introduce the local Boltzmann difference (3.29):

$$f(x^\mu, p^\mu) \propto n(x^\mu) \exp(-E^*/T),$$

which describes the local equation. Let us use the formula (3.50) and the assumption: $n(x^\mu) = \rho(r)$, which means that the density profile depends only on the radial coordinate. If we move to other coordinates, the left-hand side is also more relevant. We're getting pretty good:

$$\frac{d3N^{(fo)}}{m_t\, dm_t\, d\varphi dy} = m\tau_{fo} \int_0^\infty dr r\rho(r) \int_0^{2\pi} d\vartheta \int_{-\infty}^{+\infty} d\eta_s \cosh(\eta_s - y) \exp(-\frac{E*}{T}) =$$

$$= m_t \tau_{fo} \int_0^\infty dr r\rho(r) \int_o^{2\pi} d\vartheta \exp(-\frac{p_t \sinh \eta_t(r) \cos(\varphi - \vartheta)}{T}) \int_{-\infty}^{\infty} d\eta_s \cosh(\eta_s - y) \exp(-\frac{m_t \cosh \eta_t(r) \cosh(\eta_s - y)}{T}). \tag{3.51}$$

In the integral, we can introduce substitutions for $(\varphi\ \vartheta)$ and $(\eta_s\ y)$, and given appropriate inte- graphical limits, then the result will not depend on φ, y. This is a characteristic property of the boost-invariant expansion. In addition, we can also introduce modified Bessel functions to replace the integrals in the conclusions.

$$\frac{d3N^{(fo)}}{m_t\, dm_t\, d\varphi dy} = m\tau_{fo} \int_0^\infty dr\, r\rho(r) I_0\left(\frac{p_t \sinh \eta_t(r)}{T}\right) K_1\left(\frac{m_t \cosh \eta_t(r)}{T}\right) \tag{3.52}$$

Starting from (3.32) and (3.52) we obtain explicitly

$$S(x, K) d^4 x = \delta(\tau - \tau_{fo}) m_t\, \rho(r) \cosh(\eta_s - y) \exp(-\frac{p\, u^\mu_{\ \mu}}{T}) \tau d\tau d\eta_s\, r dr d\vartheta. \tag{3.53}$$

Recall that $r = \sqrt{x_1^2 + x_2^2}$ is a radial coordinate, to introduce the assumptions:

$$\rho(r) = \Theta(R - r) \qquad\qquad \eta_t = \sqrt{2}\eta_f \frac{Rr}{}. \tag{3.54}$$

This means that we assume a homogeneous distribution of the particle number density in the case of the freeze-out with radius R and a linear increase in the fireball velocity with increasing radial coordinate, ...which is explained by the increase in the con- stant pressure. We retain η_f as a parameter that corrects the intensity of the transverse flow. Using this model, we can calculate (3.39) and compare the results with the experiment. In addition, we can fit the assumptions in (3.52), where we can integrate the expression of φ and go from m_t to p_t and explicitly check:

$$\frac{d^2N^{(fo)}}{2\pi p\, dp_{tt}\, dy} = m_t \tau_{fo} \int_0^R Dr\, r I_0 \left(\frac{p_T \sinh\left(\sqrt{r\_}\, 2\eta_f \frac{R}{}\right)}{T} \right) K_1 \left(\frac{m_T \cosh\left(\sqrt{r\_}\, 2\eta_f \frac{R}{}\right)}{T} \right) . \quad (3.55)$$

We can also adjust the shape:

$$\frac{d\, N^{2(fo)}}{2\pi p_t\, dp_t\, dy} = \frac{\tau R_{fo}}{\sqrt{2}\eta_f} m_t \int_0^{\sqrt{2}\eta_f} ds\, s\, I_0 \left(\frac{p_t \sinh(s)}{T}\right) K_1 \left(\frac{m_t \cosh(s)}{T}\right) . \quad (3.56)$$

The problem with this spectrum estimate is that it is very difficult to include the significant effect of resonance decay. For this reason, the program DRAGON was developed to correct this handicap by means of the Monte Carlo method. See Section 4. The procedure and results of the numerical integration in Sections A.1, A.2.

3.7.1 Areas of homogeneity

From the nature of the local thermalization of the expanding fireball $\frac{d^3N}{d^3p} \propto \rho(r) \exp(-p\, u_\mu^\mu / T)$ it is evident that each moving part of the fireball produces a momentum with a temperature difference in its rest frame. Therefore, by observing certain momenta, we will locate certain regions of the fireball that produce most of the particles with this momentum. These regions are called homogeneity regions. By further considerations, the following approximate dependencies can be derived [3]:

$$R_{long} = \tau_{fo} \sqrt{\frac{T}{K_t^2 + m^2}},$$

$$R_s = \frac{R_{\mathcal{I}}^2}{1 + M_t \eta_f / T}.$$

These quantities measure the size of the homogeneity region, i.e., a certain part of the fireball.

3.7.2 Slope of the spectrum of the forward momentum, freezing temperature

For the analysis of the spectrum in the forward momentum we introduce the following quantity:

Slope of the přícný momentum spectrum: $T_{slope} = \left(-\partial_{m_t} \ln \frac{d^3 N}{m_t dm_t d\theta dy} \right)^{-1}$.

For limiting cases we have analytical results

$$T_{slope} = T_{fo} \sqrt{\frac{1+\langle v_t \rangle}{1-\langle v_t \rangle}} \quad \text{ultra-relativistically}, \quad p_t\, m$$

q

$$\square, T_{fo} + m < v_t >^2 \qquad \text{non-relativistic}' \quad p_t << m,$$

where T_{fo} is the freezeout temperature. Increasing T_{fo} and η_f leads to a decrease in T_{slope} and thus to a flatter spectrum. *The spectrum is generally better described by the second relation.* We [illegible] that the slope
the spectrum will depend on the mass of the particle, as in the non-relativistic case.

If we want to determine T_{slope} with the measure T_{fo}, we have to calculate the spectrum of the same heart for two different types of particles with different masses m, assuming they have the same T_{fo}, which is not a trivial assumption. Since the interaction between the nucleons takes place at lower temperatures at a higher pion, it is reasonable to assume that the nucleon-pion system is well [illegible] even when the cross-section is not well differentiated.

Chapter 4

Simulation in DRAGON

4.1 The DRAGON program and its parameters

For the calculations, I used the Dragon [9] program, which uses the Blastwave model to simulate the central energy sources based on the input parameters of the model using the Monte Carlo method. The program proceeds by generating the position of the fireball origin and using (3.47) to calculate the velocity at^{μ} of a given fireball. Then it generates the energy according to the difference (3.29) and the direction is isotropic. It boosts the resulting city according to $^{\mu}$. The DRAGON program also includes the production of resonances and their subsequent decay into stable particles.

Due to the inherent boost-invariance of the spectrum in the forward momentum of the Blastwave model, there is no need for the interval of the acceptance of the particles into the statistics at a rate $y < P$, where P is the constant determining this interval, corresponds more closely to the interval used in the experiment. However, it is also necessary to consider the range of the simulated *double maxrap* spectrum. To
the difference of the goodness of fit corresponds to the boost invariant, $P/maxrap <$ you need to ensure at least $1/5$. I have applied these considerations in later fitting of the experimental data.

This program was run with the following parameter settings in the rams.hpp file":

NOEvents= 14000 double DropletPart = 0..;
double fotemp = 0.04 and 0.13; double etaf = 0.3 aˇz
1.2; double Tch = 0.1656 double mub = 0.028;
double mus = 0.0069 ; double huen = 0.7;
double minrap = -5..; double maxrap = 5th ;
double N_total = 4.5 * 9000 ; double rapcenter = 0.0;
double rapwidth = 1.4; double rb = 10..;
double a_space = 1.0; double tau = 9..;
double rho2 = 0.0; double tau = 9.;
int NOSpec = 277;

An explanation of the parameters can be found in the literature [9] „pa-

4.2 Programme editing

In order for the program to efficiently implement the requirements set in this work, several adjustments had to be made.

The original DRAGON is conceived in such a way that it generates the particles based on the Blastwave model using the Monte Carlo method with fixed input parameters. The information about the generated data is stored in a file. The problem is the considerable size of the resulting files due to the state statistics. So is the need for data processing. Since this process involves many operations of computing and saving to disk, it is necessarily a very slow process, but the end result is a file of several kilobits in size containing the typical spectrum of interest. Such a concept is unsuitable for repeated calculations of the same type, which are necessary, for example, when fitting the input parameters of a model. Therefore, I have made some modifications to the program for the purpose of my study:

1. I have added a custom library for working with matrices in C++ based on dynamic arrays (size determined per run) and templates (allows to write libraries independent of the types of variables used).
2. I have added my own library for histogram creation while running the program using the above mentioned libraries for working with matrices. This avoided an entire intermediate step that slowed down the process. The bin boundaries in the histogram are automatically calculated from the set of experimental values, which is useful for later comparison of results.
3. In order to speed up the calculation, I created a simple bash script that uses the independence of the individual calculations and parallelizes them. For this I used the Grid Engine program on the Sunrise Cluster workstation.
4. I have implemented a program for data analysis using χ^2 (η_f, T_{fo}) spectra from DRAGON and from the experiment. The values of χ^2 are then stored in a file as a matrix. The search minimum can then be easily isolated and a fit to the experimental data can be performed.

The search for the minimum χ^2 for various parameters η_f and T_{fo} is carried out as follows:

1. Cycle
   (a) setting of the parameters η_f and T_{fo}
   (b) running DRAGON with given parameters
   (c) ˇc´astic generation by DRAGON and histogram filling for the spectrum in p_T
2. Calculate χ^2 (η_f, T_{fo}) of the normalized values with respect to the experimental data
3. Write χ^2 (η_f, T_{fo}) into the table

4. Find the minima in the table χ^2 (η_f, T_{fo}).

4.3 Results of calculations

4.3.1 Experimental data, data normalization

I used the data from the STAR experiment [10], specifically the invariant spectra in the příčné momentum $dN^2/(2\pi p_T\, dp_T\, dy)[(GeV/c)^{-2}]$ versus p_T [GeV/c] Au+Au srážek při rapiditě $y < 0.1$ and centrality 5 6% for 6 types of particles and 3 different energies: p, $\bar{p}$, $\pi^{\pm}$, $K^{\pm}$ at 62.4, 130 and 200 GeV per nucleon.

I have used the approximation of the independence of the spectrum from the rapidity, which is appropriate in the region of the mean rapidity $y = 0$. Thus, I have actually replaced $dy = 2 * 0.1$. Since the centre of the beam is primarily the parameters η_f and T_{fo} and the normalisation of the spectrum can be corrected by the fireball radius R, which was not used, I could normalise přeškalovat as needed (see Sect. Therefore, I normalized the data so that $N_{norm}(i, j, E, T_{fo}, \eta_f)$ for individual bins lies in the interval (0, 100). In the following way:

1. I took one non-normalized spectrum $\frac{dN^2}{2\pi p_T\, dp_T\, dy}(i, j, E, T_{fo}, \eta_f)$ from program DRAGON or from experimental data for one of the i-th type of particles
2. Calculate the norm $A = \sum_j \frac{dN^2}{2\pi p_T\, dp_T\, dy}(i, j, E, T_{fo}, \eta_f) * (p_T)_j\ [GeV/c]$, where the sum prochází all the bins in the histogram and $(p_T)_j$ [GeV/c] is the total momentum of the j-th bin in GeV/c
3. Using this I defined $N_{standards}(i, j, E, T_{fo}, \eta_f) = \frac{100}{A} * \frac{dN^2}{2\pi p_T\, dp_T\, dy}(i, j, E, T_{fo}, \eta_f)$

4.3.2 Calculate χ^2 to fit the parameters T_{fo} and η_f

To fit the parameters of the Blastwave model, I have calculated χ^2 for the individual settings of the parameters T_{fo} and η_f and the individual energies by the following relation:

$$\chi^2(E, T_{fo}, \eta_f) = \sum_{(castice)_i} \sum_{(p_T)_j} \frac{\left(Nnorm_{.DRAGON}(i, j, E, T_{fo}, \eta_f) - Nnorm_{.exp.}(i, j, E)\right)^2}{\sigma norm_{.exp}(i, j, E)^2},$$

where the first sum passes through all analyzed types of particles and the second sum passes through all bins in p_T. I entered the data into the following table and 2D graph and found the minima for all 3 energies:

E [GeV]	η_f	T_{fo} [GeV]	χ^2_{min} (E)
62,4	0,8	0,08	2,66
130	0,8	0,08	2,35
200	0,9	0,08	0,81

Table 4.1: Values of the parameter η_f , T_{fo} [GeV] for finding the minima of the function χ^2 (η_f, T_{fo}) (see Subsection 4.3.2) and for different energies see also the tables in Section A.3.

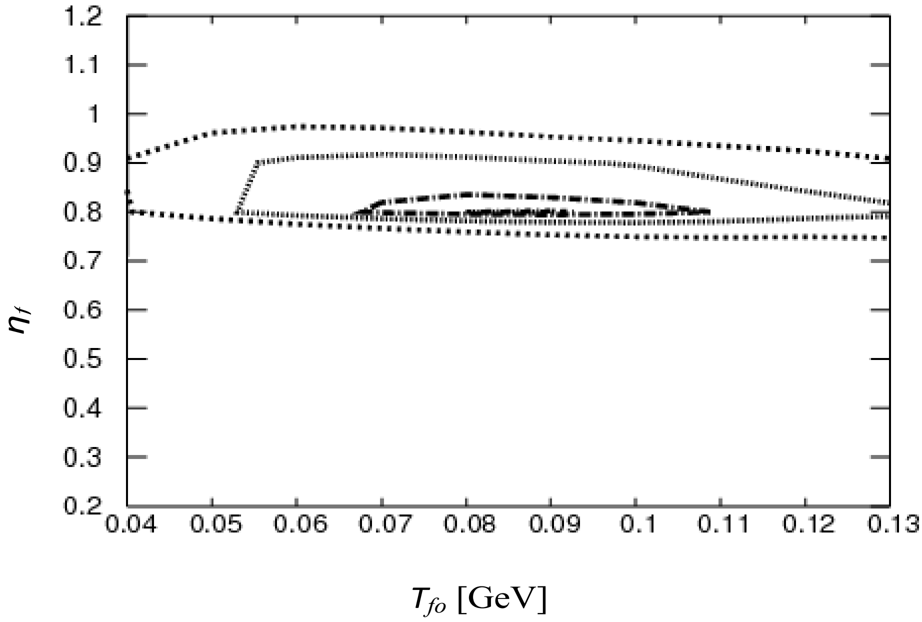

Figure 4.1: The 1σ, 2σ and 3σ contours around the found minimum of the function χ^2 (η_f, T_{fo}) of the normalized data from the Monte Carlo generator DRAGON and the experiment $dN^2/(2\pi p_T\, dp_T\, dy)[(GeV/c)^{-2}]$ versus p_T [GeV/c] Au+Au collision at intermediate rapidity
$|y| < 0.1$ and centrality 5 - 6% for p, $\bar{p}$, $\pi^{\pm}$, $K^{\pm}$ at 62.4 GeV per nucleon [10]

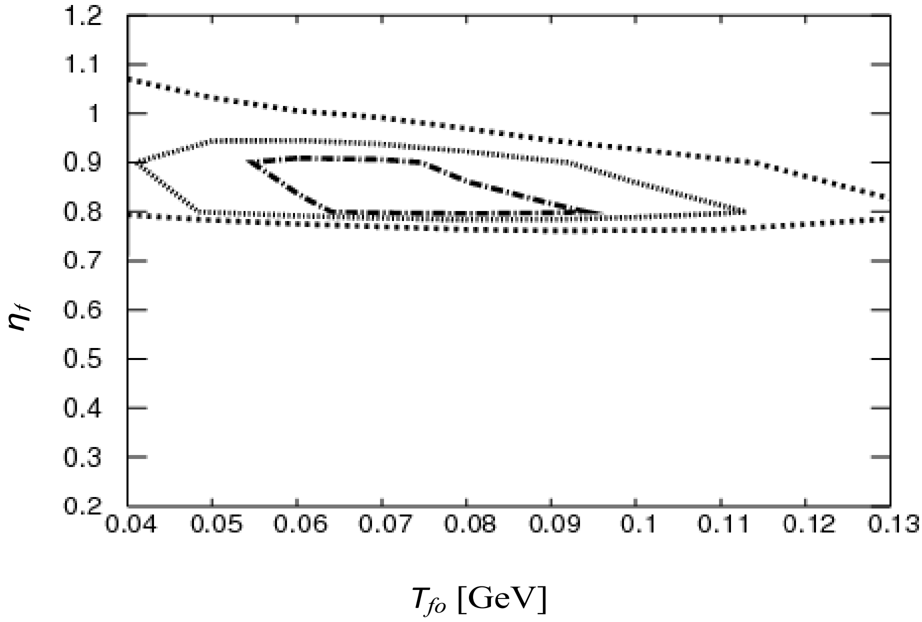

Figure 4.2: The 1σ, 2σ and 3σ contours around the found minimum of the function χ^2 (η_f, T_{fo}) of the normalized data from the Monte Carlo generator DRAGON and the experiment $dN^2/(2\pi p_T\, dp_T\, dy)[(GeV/c)^{-2}]$ versus p_T [GeV/c] Au+Au collision at intermediate rapidity
$|y| < 0.1$ and centrality 5 - 6% for p, $\bar{p}$, $\pi^{\pm}$, $K^{\pm}$ at 130 GeV per nucleon [10]

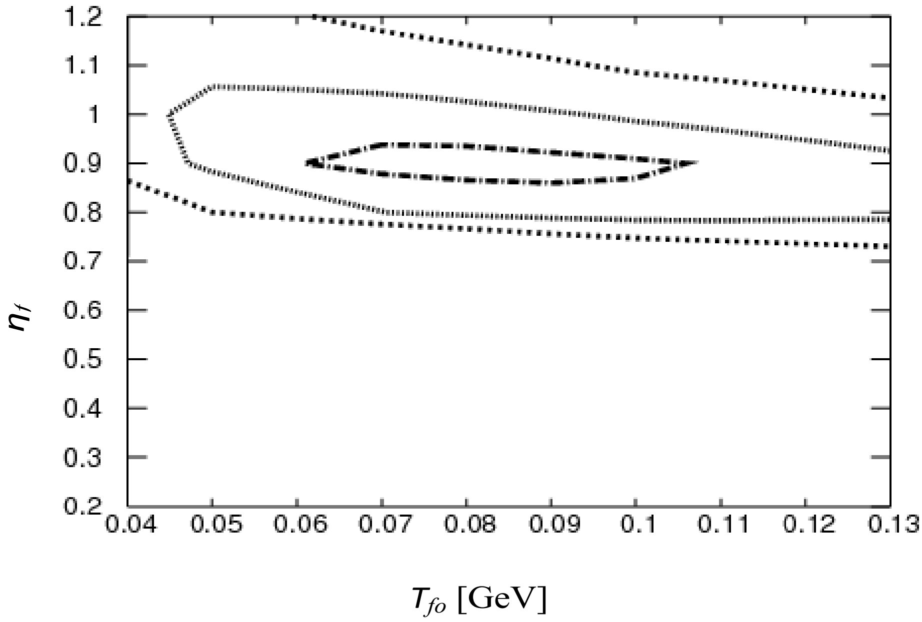

Figure 4.3: The 1σ, 2σ and 3σ contours around the found minimum of the function χ^2 (η_f, T_{fo}) of the normalized data from the Monte Carlo generator DRAGON and the experiment $dN^2/(2\pi p_T\, dp_T\, dy)[(GeV/c)^{-2}]$ versus p_T [GeV/c] Au+Au collision at intermediate rapidity
$|y| < 0.1$ and centrality 5 - 6% for p, $\bar{p}$, $\pi^{\pm}$, $K^{\pm}$ při 200 GeV per nucleon [10]

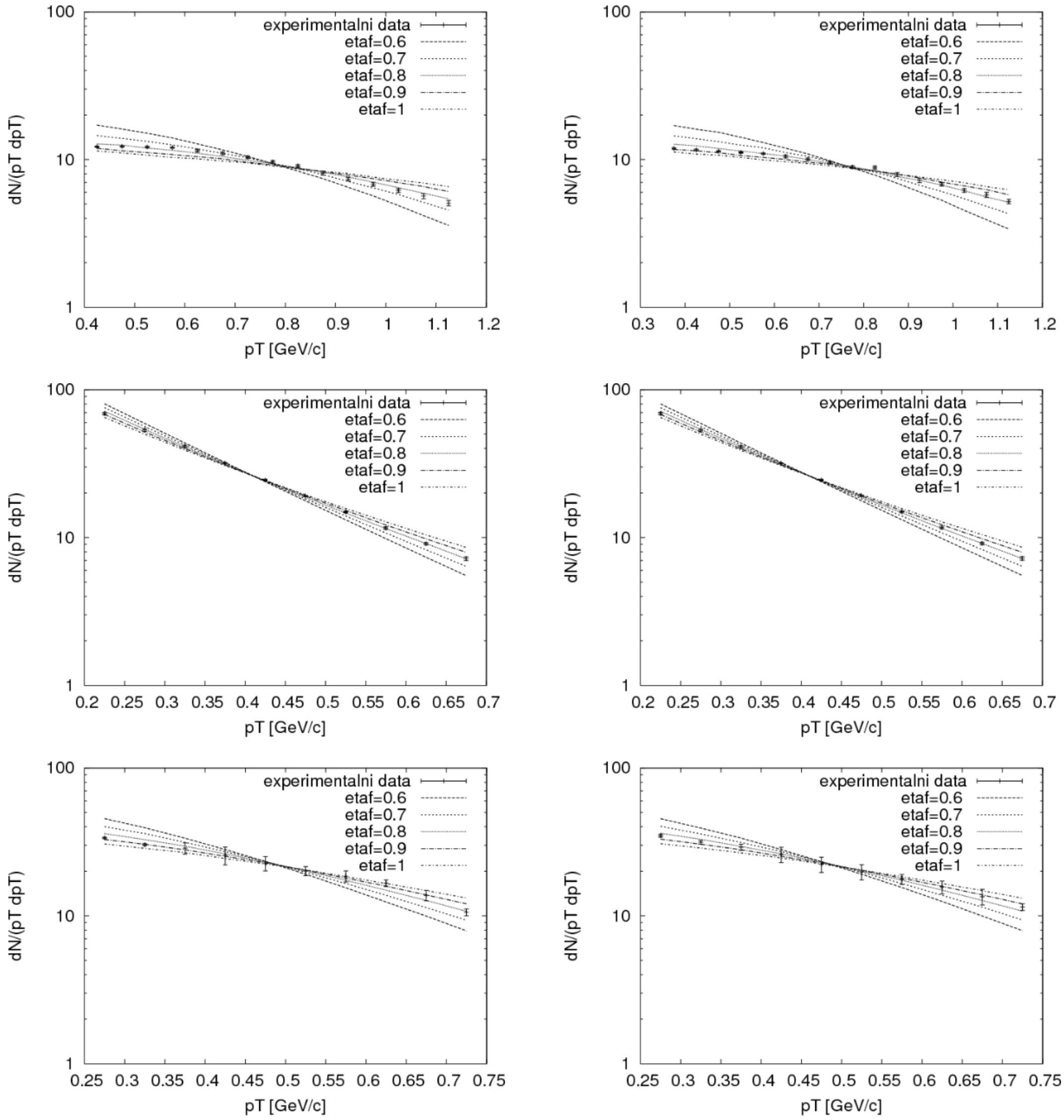

Figure 4.4: Spectra in the pˇr´ıˇc´ıc´ı momentum of the normalized DRAGON data at T_{fo} = 0.08 GeV and the experiment $dN^2/(2\pi p_T\ dp_T\ dy)[(GeV/c)^{-2}]$ versus p_T [GeV/c] Au+Au Sr´ıˇzek þ] at stˇmedium rapidity $y < 0.1$ and centrality 5 6% for the ˇc´ particles from top left to right in the following order p, $\bar{p}$, π^-, π^+, K^-, K^+ at 62.4 GeV per nucleon [10]

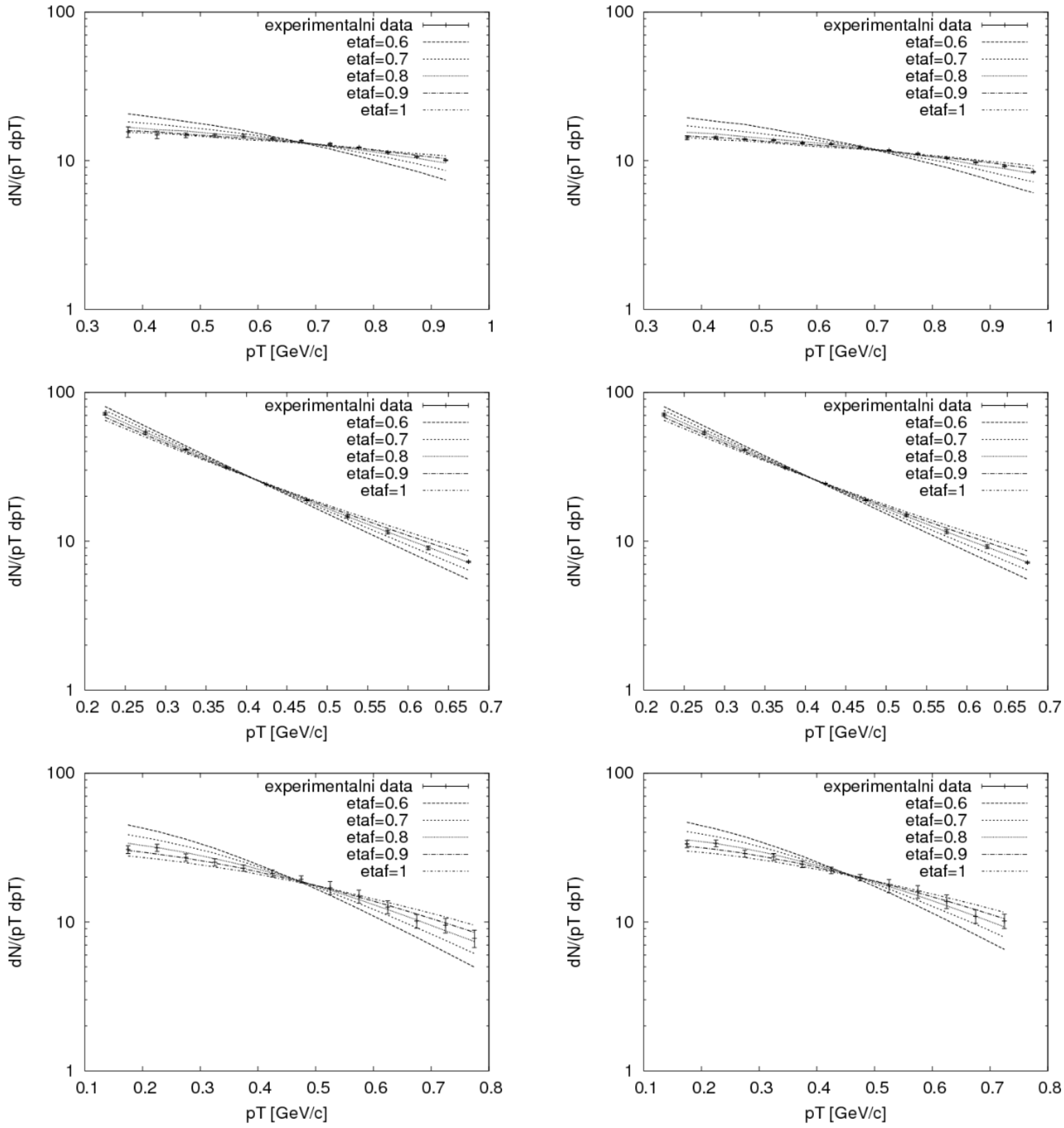

Figure 4.5: Spectra in the pˇr´ıˇc´ıc´ı momentum of the normalized DRAGON data at $T_{fo} = 0.08$ GeV and the experiment $dN^2/(2\pi p_T\, dp_T\, dy)[(GeV/c)^{-2}]$ versus p_T [GeV/c] Au+Au Sr´ıˇzek pˇ] at stˇmedium rapidity $y < 0.1$ and centrality 5 6% for the ˇc´ particles from top left to right in the following order p, $\bar{p}$, π^-, π^+, K^-, K^+ at 130 GeV per nucleon [10]

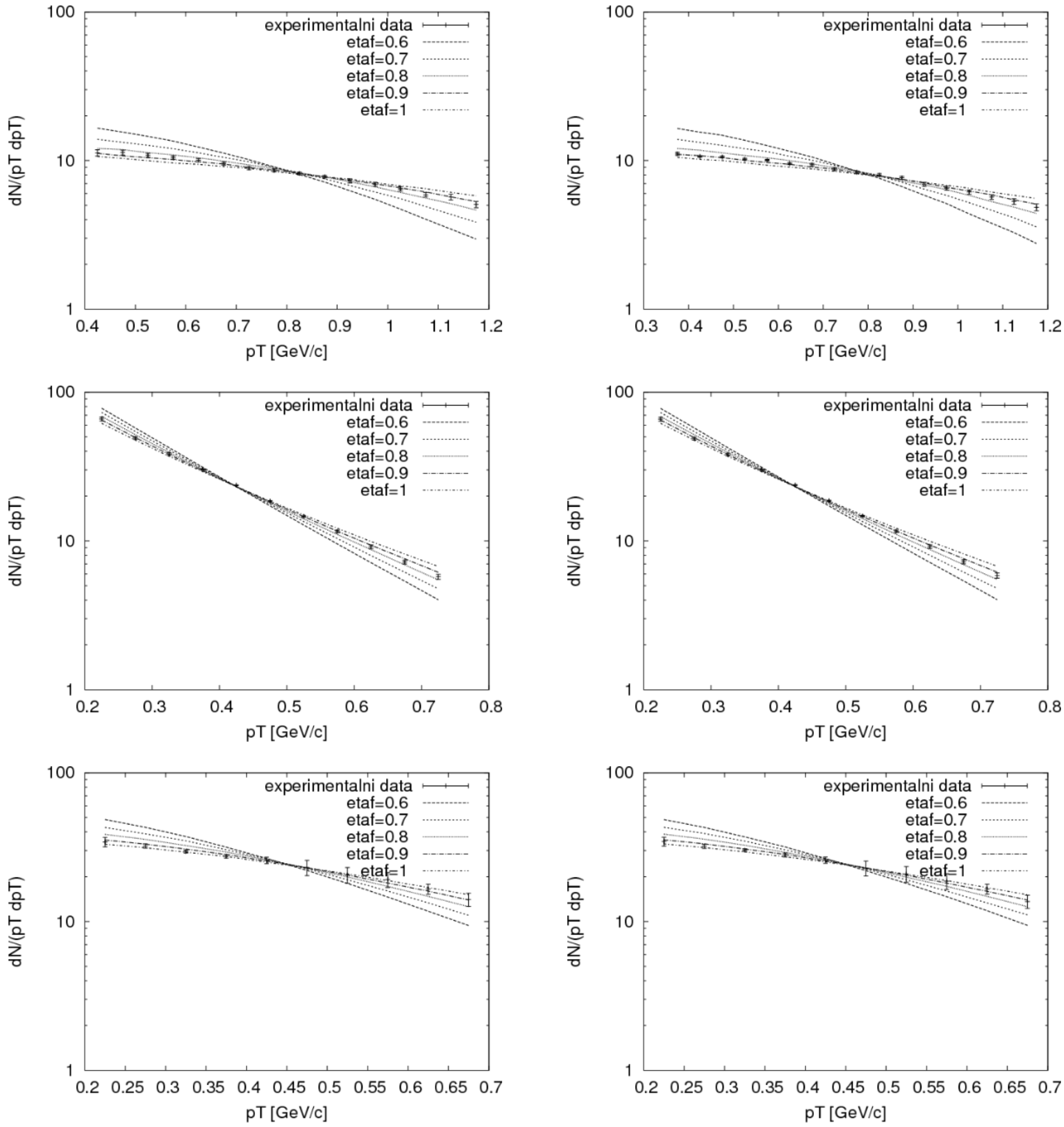

Figure 4.6: Spectra in the pˇr´ıˇc´ıc´ı momentum of the normalized DRAGON data at T_{fo} = 0.08 GeV and the experiment $dN^2/(2\pi p_T\, dp_T\, dy)[(GeV/c)^{-2}]$ versus p_T [GeV/c] Au+Au Sr´ıˇzek pˇ at stˇmedium rapidity $y < 0.1$ and centrality 5 6% for the ˇc´ particles from top left to right in the following order p, $\bar{p}$, π^-, π^+, K^-, K^+ at 200 GeV per nucleon [10]

Závěr

By means of a software modifications some outputs the DRAGON program [9], I fit the two most important parameters of the Blastwave model with resonances to the normalized (see subsection 4.3.1) spectra in the higher momentum from the STAR experiment [10]:

E [GeV]	η_f	T_{fo} [GeV]	$\chi^2_{min}(E)$
62,4	0,8	0,08	2,66
130	0,8	0,08	2,35
200	0,9	0,08	0,81

Table 4.2: Values of the parameter η_f , T_{fo} [GeV] for finding the minima of the function χ^2 (η_f, T_{fo}) (see subsection 4.3.2) and for different energies see also the tables in section A.3.

Interestingly, when the spectra for the fitted values are quite consistent (see the graphs in subsection 4.3.2), the values of the freezing temperature T_{fo} are roughly half of the previous estimates [15, 16, 17, 18]. There are several explanations:

If the chosen parameters are [illegible] they must be taken into [illegible] with the others.

The region in the higher momentum that I have analysed is too narrow.

It is necessary to adjust the parameter for the chemical composition for the energy 62.4 [GeV].

The choice of the Blastwave model's frosting surface is not [illegible]

A possible continuation of this work would be to add as additional data the results symmetrization effect - HBT interferometry, see subsection 3.6.

List of sources used

[1] F. Cooper and G. Frye, Phys Rev. D 10 (1974) 186.

[2] J. D. Bjorken, Phys. Rev. D 27 (1983) 140.

[3] T. Cs¨org˝o and B. Lörstad, Phys. Rev. Rev. C 54 (1996) [arXiv:nucl-th/9901094].

[4] E. Schnederman, J. Sollfrank and U. Heinz, Phys. Rev. Rev. C 48 (1993) 2462 [arXiv:nucl-th/9307020].

[5] J. Letessier and J. Rafelski, *Hadrons and Quark-Gluon Plasma*, textbook, Cambridge monographs on particle physics, nuclear physics and cosmology

[6] U. A. Wiedemann and U. Heinz, Phys. Rept. 319 (1999) 145 [arXiv:nucl-th/9901094].

[7] C.-Y. Wong, Introduction to High-Energy Heavy-Ion Collisions, World Scientific, 1994.

[8] Boris Tomášik, Diploma thesis, MFF Komensk´e University 1995.

[9] B. Tomasik, Comp.Phys.Commun. 180 (2009) 1642-1653.

[10] B. I. Abelev et al [STAR Collab.] Phys. Rev. C 74 (2009) 034909.

[11] File:Standard Model of Elementary Particles.svg #file In Wikipedia : the free encyclopedia [online]. St. Petersburg (Florida) : Wikipedia Foundation, 27 June 2006, 27 June 2009 [cited 2010-04-06]. Available from WWW: http://en.wikipedia.org/wiki/File:Standard _Model _of _Elementary_ Particles.svg# file .

[12] A. Chodos, R.L. Jaffe, K. Johnson, C.B. Thorn, V.F. Weisskopf, Phys. Rev. Rev. D 9 (1974) 3471

[13] P.J. Siemens, J.O. Rasmussen, Phys Rev. Lett. 42 (1979) 880

[14] E. Shuryak, Phys. Lett. B 78 (1978) 150

[15] W. Broniowski, W. Florkowski, Phys. Rev. Lett. 87 (2001) 272302.

[16] W. Broniowski , M. Chojnacki, W. Florkowski , A. Kisiel, Phys.Rev.Lett.101 (2008) 022301.

[17] M. Csanad, T. Csorgo , B. Lorstad , A. Ster, Acta Phys.Polon.B35 (2004) 191, e-Print: nucl-th/0311102.

[18] M. Csanad, T. Csorgo, B. Lorstad, A. Ster, J.Phys.G 30 (2005) S1079, e-Print: nucl-th/0403074.

Přílohy

A.1 Script for MATLAB for the numerical integration of the relation for the spectrum of continuously produced particles

```
e=2.71828;%basic constant
pi=3.141592654;

T=80; %MeV/k - Blastwave model parameters
etaf=0.8;

m=493; %MeV - mass of the particle


k1=@(y,t) cosh(y).* e.^(-cosh(y).*t); % work function
i0=@(y,t) e.^(-cos(y).*t); %other spectrum


maxpt=725; %define the area to be read minpt=275;
n=10;
step=(maxpt-minpt)/(n-1);

Y=1:n; %working variables
X=1:n;
spc=ones(n,2);
norm=0;

for k = 1:n
   pt=minpt+step*(k-1); %MeV/c
   mt=sqrt(pt^2 + m^2);%MeV/c2

   X(k)=pt;
   %follows triple numerical integration
   Y(k)= mt*triplequad(@(r,y,z)     r.*         i0(z,  (pt*sinh(r))/T )    .*
k1(y,  (mt*cosh(r))/T )           ,0,etaf*sqrt(2),-5,5,0,2*pi);

         spc(k,1)=X   (k)/1000; %data for saving to file pt[GeV]
         spc(k,2)=    Y(k);
         norm=norm+(X(k)/1000)*Y(k);    %working variable for
                 %normalize( take pt[GeV])
end

for k = 1:n %normalization of
    spectrum Y(k)=
    Y(k)*100/norm; spc(k,2)=
                Y(k);
end

%output of
plot(X,Y);
save('numspc.xls', 'spc', ' -ascii', '-double', '-tabs')
```

A.2 Comparison of the spectra numerically calculated for the directly produced particles, from the experiment and from DRAGON

In the following plots I compare the normalized spectra numerically obtained from (3.56) using MATLAB for the spectra of the directly produced particles from the STAR experiment and the spectra from the DRAGON program using Monte Carlo to include the resonance in the Blastwave model.

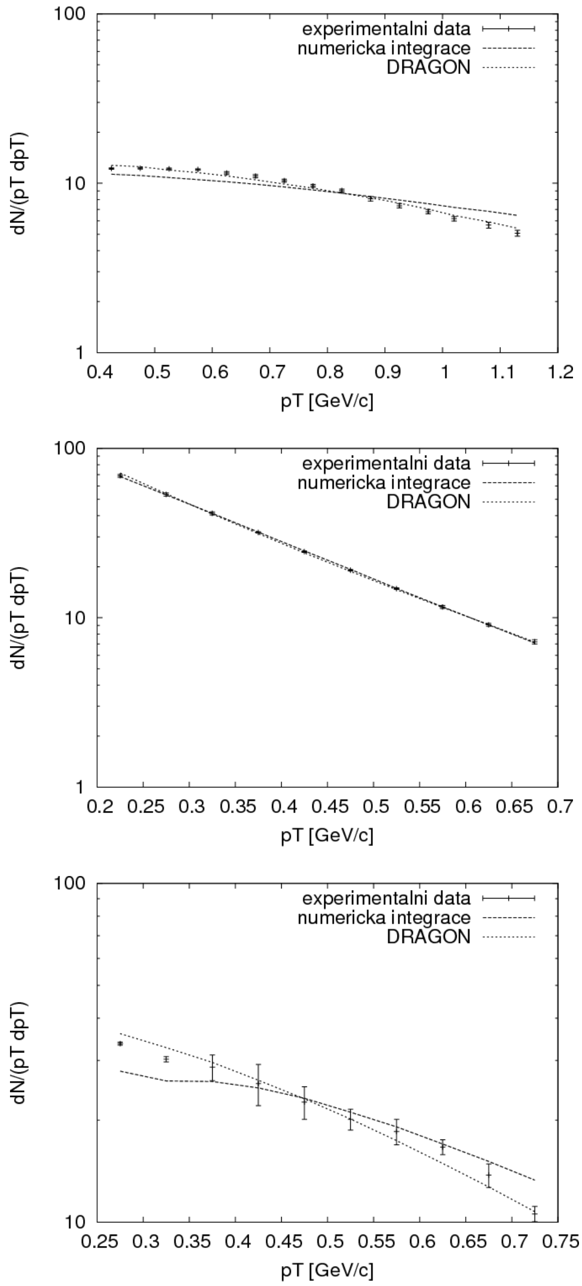

Figure A.7: Comparison of spectra in the forward momentum of normalized data from numerical integration (3.56) using MATLAB, DRAGON for $\eta_f = 0.8$ and $T_{fo} = 0.08$ [GeV] and the experiment $dN^2/(2\pi p_T\, dp_T\, dy)[(GeV/c)^{-2}]$ versus p_T [GeV/c] Au+Au sr´aˇzek pˇri midrapidit´e $y < 0.1$ and centrality 5 6% for the ˇc´asticity from above in the following order: p, π^-, K^- at 62.4 GeV [10]. The differences in the spectra (3.56) using MATLAB and DRAGON are due to the error from the resonance decay in (3.56)

A.3 Tables of results $\chi^2 (E, \eta_f , T)_{fo}$

T_{fo} [GeV]

η_f	0,04	0,05	0,06	0,07	0,08	0,09	0,1	0,11	0,12	0,13
0,3	2517,78	2042,87	1681,94	1388,15	1154,58	976,22	822,25	701,68	596,88	513,21
0,4	1303,56	1069,94	890,24	744,72	627,92	539,44	459,14	397,77	342,63	299,39
0,5	549,21	464,72	393,36	337,55	290,43	251,58	218,49	190,59	166,84	146,41
0,6	181,35	158,10	138,74	120,73	105,22	93,21	81,46	73,12	65,25	58,48
0,7	44,85	38,85	32,74	28,53	25,04	22,25	20,26	18,86	18,10	16,94
0,8	11,94	7,48	4,75	3,32	2,66	2,57	2,91	3,76	4,91	5,76
0,9	11,30	7,65	5,80	5,08	5,51	6,26	6,88	8,05	9,05	10,75
1	15,28	14,16	13,68	14,27	15,21	16,38	17,42	18,51	19,84	21,10
1,1	18,87	20,34	21,44	22,95	24,77	26,49	28,58	29,60	31,25	32,25
1,2	22,78	25,99	28,33	30,66	33,11	34,95	37,28	38,63	40,92	41,83

T_{fo} [GeV]

η_f	0,04	0,05	0,06	0,07	0,08	0,09	0,1	0,11	0,12	0,13
0,3	1428,58	1231,94	1068,82	925,34	799,85	697,95	608,45	531,45	464,20	408,56
0,4	879,82	755,39	652,30	564,19	488,33	428,48	374,88	329,98	289,57	257,55
0,5	437,53	380,07	332,15	290,25	252,19	223,28	196,47	173,80	154,67	137,17
0,6	162,42	147,31	130,12	115,63	102,13	91,78	81,85	73,46	67,65	60,73
0,7	40,93	37,95	33,83	30,71	27,17	24,72	23,16	21,25	21,52	21,19
0,8	9,23	5,80	3,79	2,69	2,35	2,82	4,09	5,70	7,82	9,67
0,9	6,62	4,01	2,61	2,80	3,97	5,97	7,89	10,44	12,72	15,77
1	9,19	9,28	10,85	12,16	14,61	17,80	20,61	23,68	26,03	28,77
1,1	12,25	15,87	20,45	22,96	26,69	30,40	34,82	36,70	40,54	43,30
1,2	17,53	23,78	30,05	34,83	38,45	43,00	48,20	50,25	55,03	57,81

Table A.3: Values of χ^2 (η_f, T_{fo}) normalized data from the Monte Carlo generator DRAGON and the experiment $dN^2/(2\pi p_T\, dp_T\, dy)[(GeV/c)^{-2}]$ versus p_T [GeV/c] Au+Au srážek při midrapidity $|y| < 0.1$ and centrality 5 - 6% for p, $\bar{p}$, $\pi^{\pm}$, $K^{\pm}$ při 62.4 GeV (first table), 130 GeV (second table) [10]

					T_{fo} [GeV]					
		0.04	0.05	0.06	0.07	0.08	0.09	0.1	0.11	0.12	0.13
η_f	0.3	1063.80	900.00	765.45	648.54	550.71	472.88	404.27	348.04	299.01	259.56
	0.4	615.40	522.71	446.06	379.86	324.02	279.86	241.13	209.59	181.53	159.11
	0.5	301.38	260.57	223.67	193.13	165.86	144.20	124.98	108.63	95.76	84.27
	0.6	122.54	107.94	93.22	80.98	69.78	61.06	53.20	46.79	41.67	36.80
	0.7	41.89	35.69	30.11	25.44	21.85	18.77	16.50	14.82	13.53	12.53
	0.8	14.34	9.84	6.83	4.89	3.77	2.99	2.64	2.80	3.26	3.51
	0.9	7.33	3.79	1.89	0.97	0.81	1.03	1.44	2.06	2.82	3.70
	1	5.74	3.83	3.28	3.21	3.70	4.49	5.36	6.09	7.02	8.05
	1.1	5.49	5.58	6.27	7.01	7.99	9.16	10.58	11.45	12.54	13.44
	1.2	6.29	7.94	9.53	11.04	12.38	13.88	15.59	16.53	17.83	18.76

Table A.4: Values of χ^2 (η_f, T_{fo}) normalized data from the Monte Carlo generator DRAGON and the experiment $dN^2/(2\pi p_T\, dp_T\, dy)[(GeV/c)^{-2}]$ versus p_T [GeV/c] Au+Au srážek při midrapiditě $|y| < 0.1$ and centrality 5 - 6% for p, $\bar{p}$, $\pi^{\pm}$, $K^{\pm}$ při 200 GeV [10]